Original Article

Role of Quercetin in Ameliorating the Histological Changes in a Rat Model of Acute Lung Injury: Histological and Immunohistochemical Study

Nehal Ahmed Dowidar, Samah Kandeel Elsayed Kandeel, Nadia Fouad Elsayed Abo Hassan and Heba Elsayed Mohammed Sharaf Eldin

Histology and Cell Biology Department, Faculty of Medicine, Tanta University

ABSTRACT

Background: Acute lung injury (ALI) leads to disrupted endothelial and epithelial barriers due to associated acute inflammation. Oleic acid (OA)-induced lung injury is a model for induction of ALI in rats. Quercetin is a flavonoid with anti-inflammatory and antioxidant actions.

Aim of the Work: This study was done to evaluate the role of quercetin in ameliorating the histological changes in a rat model of acute lung injury through using histological and immunohistochemical techniques.

Materials and Methods: Forty-eight albino rats (200 - 250 grams; 8-9 weeks), were divided into three main groups. Group I (Control group), Group II (ALI-induced group): Eight rats received single injection of 50 µL OA dissolved in 1% BSA via rat tail vein, Group III: Sixteen rats received OA as group II, then divided into Subgroup IIIA& Subgroup IIIB: rats received 10 &50 mg/kg quercetin orally daily for 21 days respectively.

Results: ALI-induced group showed thickened interalveolar septae, interstitial& perivascular inflammatory cellular infiltrations, congested blood vessels, disorganized alveoli with intra-alveolar and interstitial hemorrhage, bronchioles with separated epithelial lining, perinuclear vacuolation and their lumen contained exudate, and interstitial areas of homogenous acidophilia at H&E sections. Besides, significant increase in the mean area percentage of CD68 positive cells. Also, prominent ultrastructural changes of type I&II pneumocytes, and pulmonary blood capillaries. Quercetin treated groups showed dose-dependent improvement in the histological structure of the lung.

Conclusion: Quercetin ameliorates ALI in rats in a dose dependent manner.

Key Words: ALI, CD68, Electron Microscopy, Oleic Acid, Quercetin.

Received: 18 September 2024, **Accepted:** 15 October 2024.

Corresponding Author: Nehal Ahmed Dowidar, Histology and Cell Biology Department, Faculty of Medicine, Tanta University. **Tel.:** +201121762136, **E-mail**: nehal.dwedar@med.tanta.edu.eg

ISSN: 2735-3540, vol. 75, No. 4, December 2024.

INTRODUCTION

Lung is a very important organ that is exposed to a wide range of external pollutants and biological materials. It is vulnerable to be at risk of getting different stages of illness affecting our quality of life or may lead to death[1]. Acute lung injury (ALI) can affect different varieties of age and it is responsible for thousands of deaths annually all over the world[2].

Oleic acid is an unsaturated fatty acid, present in plants and animals. Oleic acid-induced lung injury is an animal model of acute lung injury. It is associated with increased capillary permeability, leading to inflammation and pulmonary edema[3-6].

Quercetin is a dietary flavonoid that is present in fruits, vegetables, seeds, nuts, and flowers. It can be found also in broccoli, dark cherries, green tea, olive oil, besides berries[7, 8]. It is used due to its strong anti-inflammatory, immunosuppressive, and antioxidant properties. Quercetin is also of beneficial effect in the management of many oxidative, inflammatory, and allergic conditions[9,10].

Thus, the current work sought to investigate the possible role of quercetin in ameliorating the histological alterations in a rat model of ALI. This is accomplished through employing different histological and immunohistochemical methods.

DOI: 10.21608/ASMJ.2024.321941.1314

MATERIALS AND METHODS

Chemicals

- Oleic Acid (OA), (ADVENT CHEMBI, Egypt) A colorless liquid form, dissolved in 1% Bovine serum albumin (BSA).
- Quercetin, (MRM nutrition, Egypt) A yellowish powder, dissolved in 0.5% carboxymethylcellulose.
- Bovine serum albumin, (ADVENT CHEMBIO, Egypt) A whitish powder, dissolved in phosphate buffer saline at concentration of 1g/100ml.
- Carboxymethylcellulose, (Alpha Chemika, Egypt) A whitish powder, dissolved in warm water at concentration of 1g/50 ml.

Animals

Forty-eight adult male albino rats, aged from 8 to 9 weeks, and weighing from 200 to 250 grams. Rats were kept in clean well-ventilated cages and allowed for water and food intake.

The experimental groups

The rats were divided into three main groups as the following:

- **Group I (Control group):** Twenty-four rats that were divided into 3 subgroups:
  - Subgroup IA: Eight rats received no treatments.
  - Subgroup IB: Eight rats received a single injection of 2 ml 1% bovine serum albumin (dissolvent of oleic acid) via rat tail vein.
  - Subgroup IC: Eight rats received 1ml of 0.5% of carboxymethyl-cellulose (dissolvent of quercetin) once daily orally by an oral gavage for 21 days.
- **Group II (Acute lung injury [ALI]-induced group):** Eight rats that received a single injection of 2 ml of 50 μL of oleic acid dissolved in 1% BSA via rat tail vein[11].
- **Group III (ALI treated with quercetin):** Sixteen rats that received oleic acid with the same dose as group II and then divided equally into further two subgroups:
  - Subgroup IIIA (ALI treated with low dose of quercetin) (ALI+QLD): after three hours of OA treatment, the rats were received 1ml of quercetin dissolved in 0.5% of carboxymethyl-cellulose at a dose of 10 mg/kg[12].
  - Subgroup IIIB (ALI treated with high dose of quercetin): (ALI+QHD): after three hours of OA treatment, the rats were given 1ml of quercetin dissolved in carboxymethyl-cellulose at a dose of 50 mg/kg[13].

Doses of quercetin of group III were given to rats once daily for 21 days by oral gavage.

Tissue preparation

At the 21st day, rats were injected with sodium pentobarbital intraperitoneally (50 mg/Kg)[14]. An incision was made in the middle of thorax and the lungs were dissected and washed with saline. Specimens from the left lower lobe of lung were split into two halves. One half was fixed in 10% formol saline and processed to get paraffin sections for light microscopic examination. While the other half was immediately fixed in 2.5% buffered glutaraldehyde and prepared for electron microscopy.

Light microscopic study

1. Haematoxylin and Eosin (H&E): Sections were cleaned, dehydrated, fixed, and impregnated. Then embedded in paraffin. Sections of 5 microns' thickness obtained by the rotatory microtome (Leica Biosystems, China) and stained by H&E[15].
2. Immunohistochemical staining of CD68 (cluster of differentiation 68): Arkhipov[16].

Sections were deparaffinized, rehydrated, washed, incubated with 10% normal goat serum, rinsed, and incubated overnight at 4°C with the primary antibody; monoclonal mouse α-CD68 antibody at a dilution of 1:50 (AbD Serotec, Inc.) (Catalog # MCA341GA) (to detect macrophages). Followed by placing in biotinylated secondary anti-mouse antibody (Vector Laboratories, Inc.) (Catalog # BA-2001) for half an hour at room temperature. Finally, using 3,3′-diaminobenzidine (DAB) and counterstaining with Mayer's hematoxylin. A positive cytoplasmic reaction for macrophages was seen. Phosphate Buffer Saline (PBS) was used as a substitute for the 1ry anti-body to provide the negative control, while the positive control for CD68 is obtained from tonsil [EPR23917-164] (ab283654).

Transmission electron microscopic study

Lung specimens were fixed in phosphate buffered glutaraldehyde, post-fixed in 1% phosphate-buffered osmium tetroxide, dehydrated and embedded in epoxy resin. Ultrathin sections (75 nm) were stained with uranyl acetate and lead citrate. Finally, specimens were examined by JEOL electron microscope at 80 KV at The Electron Microscope Unit of Faculty of Medicine, Tanta University[17, 18].

Morphometric study

Photographs were taken using a light microscope (DM500, Leica, Switzerland) with a digital camera (ICC50, Leica, Switzerland) at Histology Department, Faculty of Medicine, Tanta University. The following parameters were measured for each group using five distinct fields from five different slides from each experimental group at a magnification power of x400 using the program Image J (National Institute of Health, Bethesda, Maryland, USA):

1. The mean thickness of the interalveolar septum at H&E-stained sections[19].

2. The mean area percentage of CD68 positive cells in the immunohistochemical stained sections of the lung.

Statistical analysis

A software, (SPSS) version 13, was used to analyze the data (SPSS Inc., Chicago, IL, USA). The Schiff test and one-way analysis of variance (ANOVA) test were used to compare the various groups with the control group. Next, the gathered information was presented as (mean ± SD). In the end, the results were deemed non-significant if $p>0.05$, highly significant if $P < 0.001$, and statistically significant if the probability value $P < 0.05$.

ETHICAL CONSIDERATION

The experiment was done in accordance with the guidelines of Faculty of Medicine, Tanta University, Egypt' Ethical Committee, with an approval Code:(36264MS27/1/2023).

RESULTS

In the present research, two rats were died, one from group II and the other one from subgroup IIIA.

Light microscopic results

1. H&E results

All control subgroups (IA, IB & IC) showed normal lung histology with alveolar ducts, alveolar sacs and alveoli interalveolar septa besides normally appeared blood vessels. Alveoli showed two types of epithelial cells. Type I pneumocytes appeared as squamous cells with flattened nuclei and type II pneumocytes appeared as dome shaped cells with rounded nuclei. The terminal bronchiole was lined with simple columnar epithelium and supporting layer of smooth muscles (Figures 1A-C).

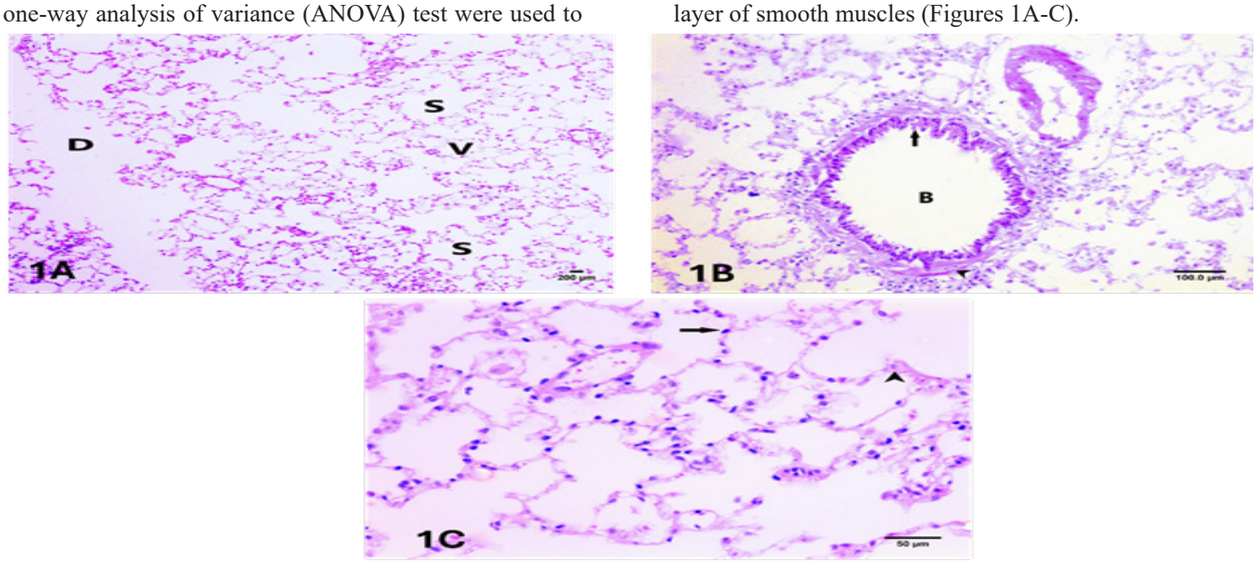

Fig. 1: H&E staining of the control group: (1A) showing alveolar ducts (D), alveolar sacs (S) and alveoli (V) [Magnification; ×100, scale bar = 200 µm]. (1B) showing a terminal bronchiole (B) lined with simple columnar epithelium (arrow) and supporting layer of smooth muscle (arrowhead) [Magnification; ×200, scale bar = 100 µm]. (1C) showing the epithelial lining of the alveoli, type I pneumocyte appeared as squamous cells with flattened nuclei (arrow) and type II pneumocyte appeared as dome shaped cells with rounded nuclei (arrowhead) [Magnification; ×400, scale bar = 50 µm].

The ALI-induced group revealed many areas of massive interstitial, and perivascular inflammatory cellular infiltrations, thickened interalveolar septae and some congested blood vessels. Many disorganized alveoli and some with intra-alveolar hemorrhage were observed. Regarding the interstitium; large homogenous acidophilic areas and interstitial hemorrhage were found. Some bronchioles showed detached epithelial lining with perinuclear vacuolation, besides exfoliated cells and exudate inside their lumen (Figures 2A-E).

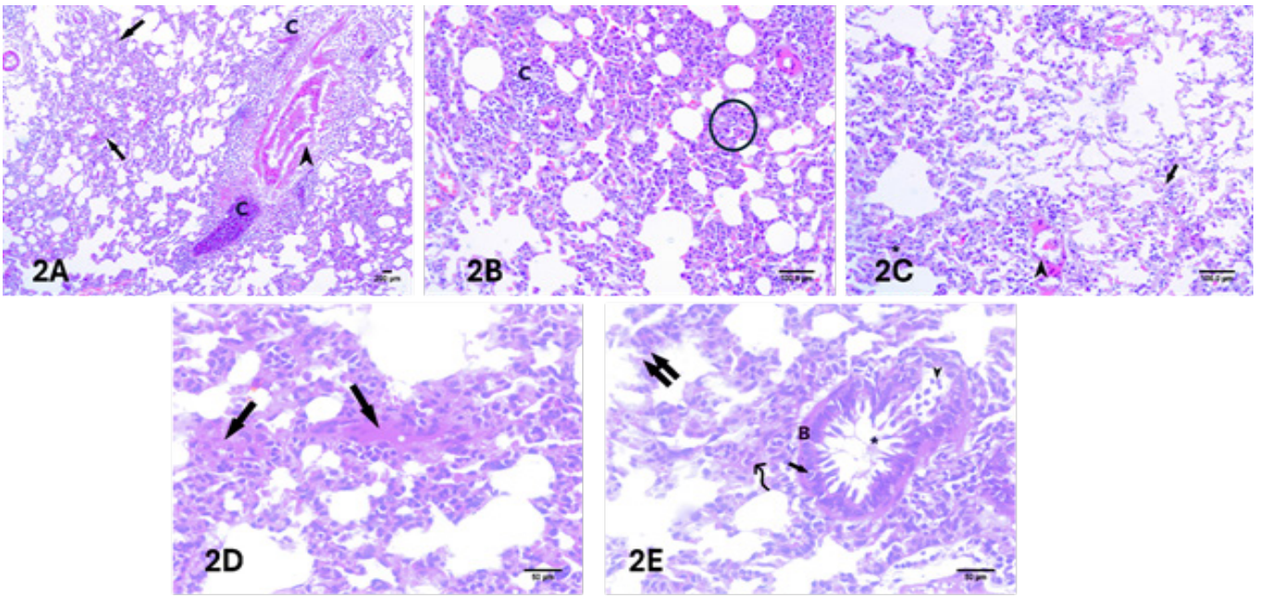

Fig. 2: H&E staining of the ALI-induced group. (2A) showing inflammatory cellular infiltrations (C) surrounding congested blood vessels (arrowhead) and thickened interalveolar septae (arrow) [Magnification; ×100, scale bar = 200 µm]. (2B) showing thickened interalveolar septae (circle) and interstitial inflammatory cellular infiltrations (C). (2C) showing many disorganized alveoli, interstitial (*), intra-alveolar hemorrhage (arrow) and congested blood vessels (arrowhead) [Magnification;(2B-2C) ×200, scale bar = 100 µm]. (2D) showing large areas of interstitial homogenous acidophilia (arrows). (2E) showing a bronchiole (B) with detached epithelial lining and exfoliated cells (arrowhead), perinuclear vacuolation (arrow), exudate (*) inside lumen, interstitial hemorrhage (double arrow), homogenous acidophilic areas (curved arrow) [Magnification;(2D-2E) ×400, scale bar = 50 µm]

Subgroup IIIA (ALI+QLD) depicted moderate improvement. Yet, small areas of interstitial and perivascular inflammatory cellular infiltrations were seen. A moderate amount of interstitial hemorrhage and some thickening of the interalveolar septae were observed. Regarding the bronchioles, they showed focal areas of detached epithelial lining (Figures 3A-C).

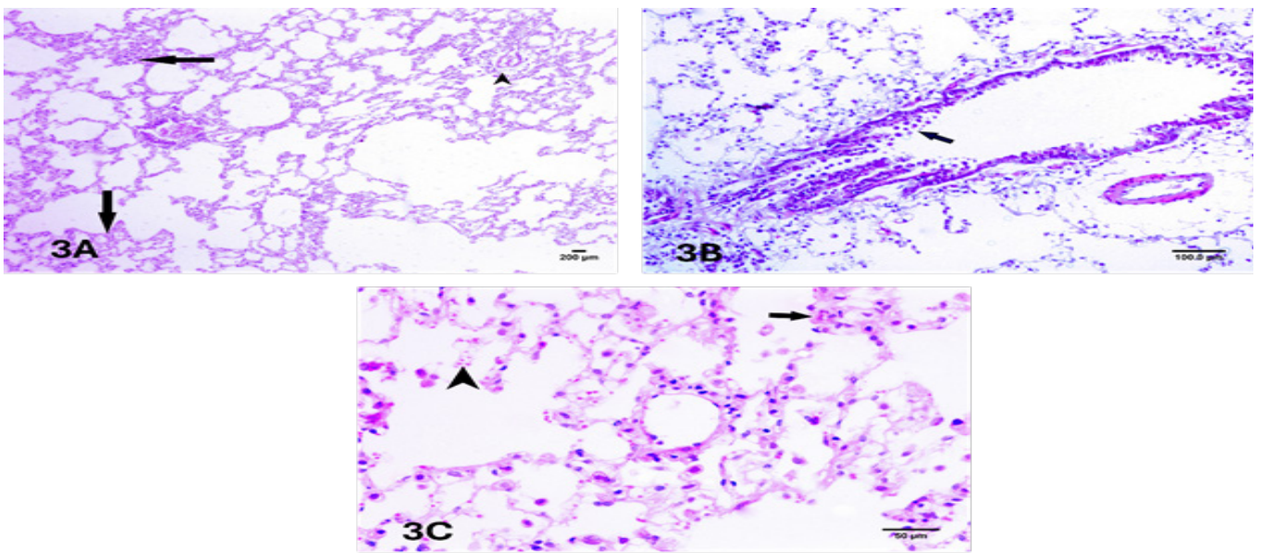

Fig. 3: H&E staining of the subgroup IIIA (ALI+QLD). (3A) showing small areas of interstitial (arrows) and perivascular (arrowhead) inflammatory cellular infiltrations [Magnification; ×100, scale bar = 200 µm]. (3B) showing bronchiole with focal areas of detached epithelial lining (arrow) [Magnification×200, scale bar = 100 µm]. (3C) showing moderate intra-alveolar hemorrhage (arrowhead) and some thickening of the interalveolar septum (arrow) [Magnification; ×400, scale bar = 50 µm].

Subgroup IIIB (ALI+QHD) showed nearly normal alveolar duct, alveolar sac, alveoli and bronchioles. Regarding the inter-alveolar septae, they appeared with apparently normal thickness. Also, type I pneumocytes appeared as squamous cells with flattened nuclei and type II pneumocytes appeared as dome shaped cells with rounded nuclei (Figures 4A-C).

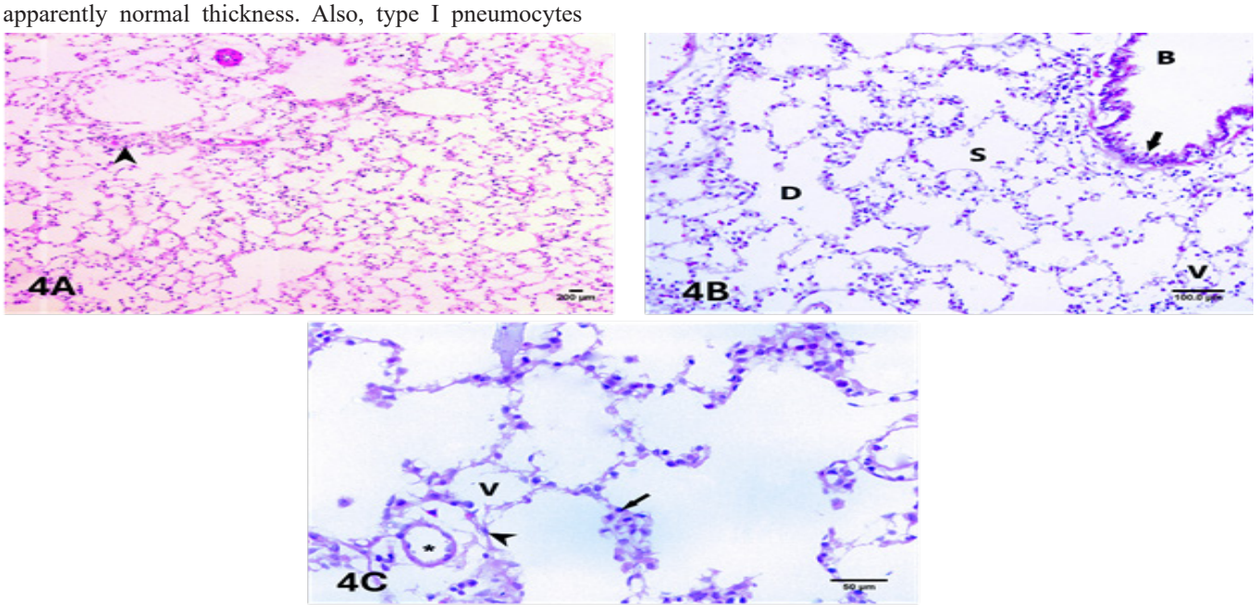

Fig. 4: H&E staining of the subgroup IIIB (ALI+QHD). (4A) showing nearly normal lung tissue with small areas of interstitial inflammatory cellular infiltrations (arrowhead) [Magnification; ×100, scale bar = 200 µm]. (4B) showing more or less normal shape alveoli (V), alveolar duct (D), alveolar sac (S) and a part of a bronchiole (B) lined with nearly normal epithelial cells (arrow) [Magnification; ×200, scale bar = 100 µm]. (4C) showing normal alveoli (V) lined intact type I pneumocytes (arrowhead) and type II pneumocytes (arrow). Notice: intact blood vessels (*). [Magnification; ×400, scale bar = 50 µm].

Regarding the mean thickness of the interalveolar septae; ALI-induced group (49.12 ± 5.45) showed a significant increase in comparison to the control group (10.22 ± 1.83). Subgroup IIIA (OA+QLD) (28.72 ± 2.05), on the other hand, demonstrated a substantial reduction in comparison to the ALI-induced group and a significant rise in comparison to the control. Subgroup IIIB (OA+QHD) (12.06 ± 1.31) exhibited a non-significant alteration in the average interalveolar septum thickness in comparison to the control group, a noteworthy reduction in comparison to the ALI-induced group, and a noteworthy decline in comparison to subgroup IIIA (Histogram 1).

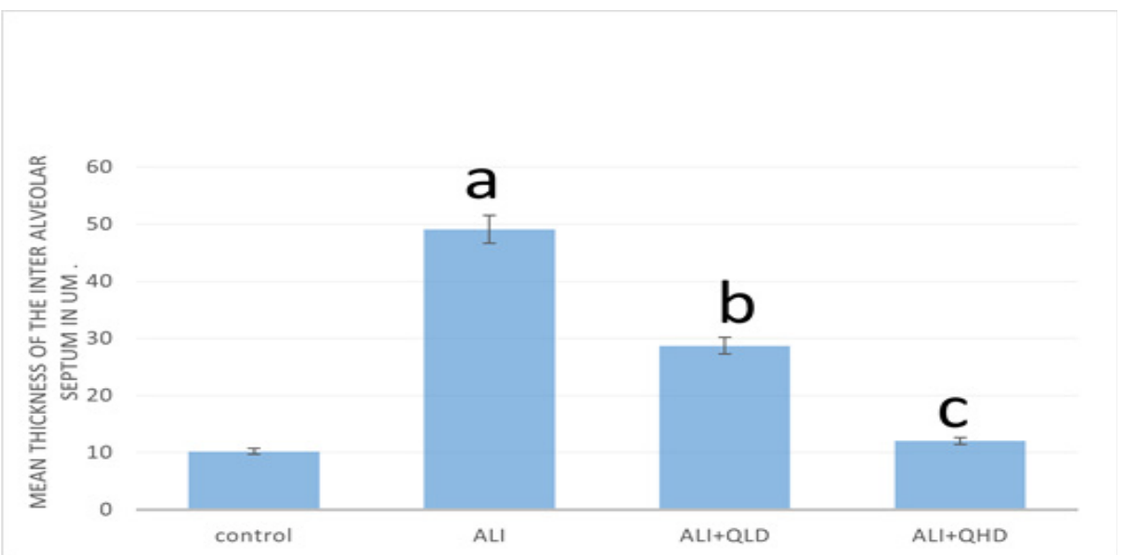

Histogram 1: The mean thickness of the interalveolar septum in the different experimental groups. Data expressed as mean ±standard deviation; ALI: acute lung injury; ALI+QLD: acute lung injury+ quercetin low dose ALI+QHD: acute lung injury + quercetin high dose
a: Highly significant increase compared to control group. b: significant increase compared to control group and significant decrease compared to ALI group c: non-significant increase compared to control group and significant decrease compared to ALI group.

2. Immunohistochemical results for CD68

Negative control of lung sections showed no immunohistochemical reaction for CD68 (5A). Positive control from the tonsil showed positive cytoplasmic reaction for CD68 (5B). Immunostained sections from all control subgroups showed a few number of macrophages with positive cytoplasmic reaction for CD68 (Figure 5C). ALI-induced group depicted numerous macrophages positive for CD68 (Figure 5D). Subgroup IIIA (ALI+QLD) demonstrated moderate number of CD68 positive macrophages (Figure 5E). Moreover, subgroup IIIB (ALI+QHD) indicated a few number of macrophages with positive cytoplasmic reaction for CD68 protein (Figure 5F).

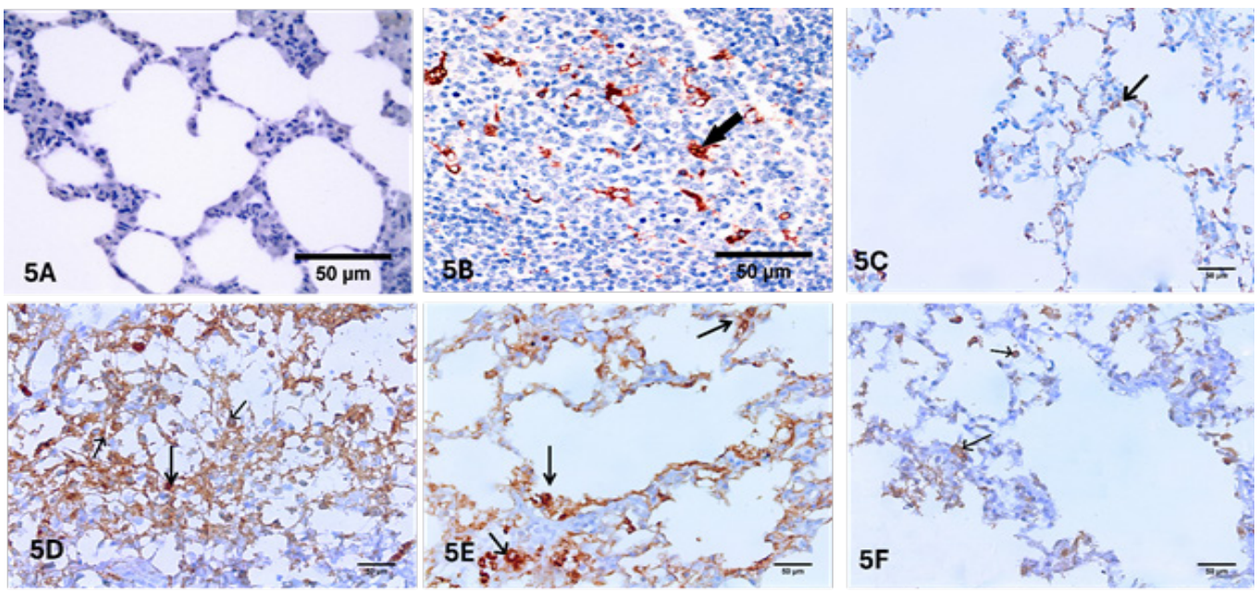

Fig. 5: CD68 immunostaining: (5A) negative control section showing no immunohistochemical reaction for CD68. (5B) positive control from tonsil showing strong positive cytoplasmic reaction for CD68 (arrow). (5C) Control group showing a few macrophages with positive cytoplasmic reaction for CD68 protein (arrow). (5D) ALI-induced group showing numerous macrophages with positive cytoplasmic reaction for CD68 protein (arrows). (5E) Subgroup IIIA (ALI+QLD) showing a moderate number of macrophages with positive cytoplasmic reaction for CD68 protein (arrows). (5F) Subgroup IIIB (ALI+QHD) showing few macrophages with positive cytoplasmic reaction for CD68 protein (arrow). [Magnification; A-F ×400, scale bar = 50 µm].

Morphometric analysis of the mean area percentage of CD68 positive cells in group II (ALI-induced group) (34.9% ± 6.55) revealed a high significant increase if compared with the control group (2.8% ± 1.03). Subgroup IIIB (7.5% ± 1.43) demonstrated a non-significant change when compared with control group and a highly significant drop when compared with group II, whereas subgroup IIIA (14.7%± 3.04) shown a substantial rise when compared to the control group (Histogram 2).

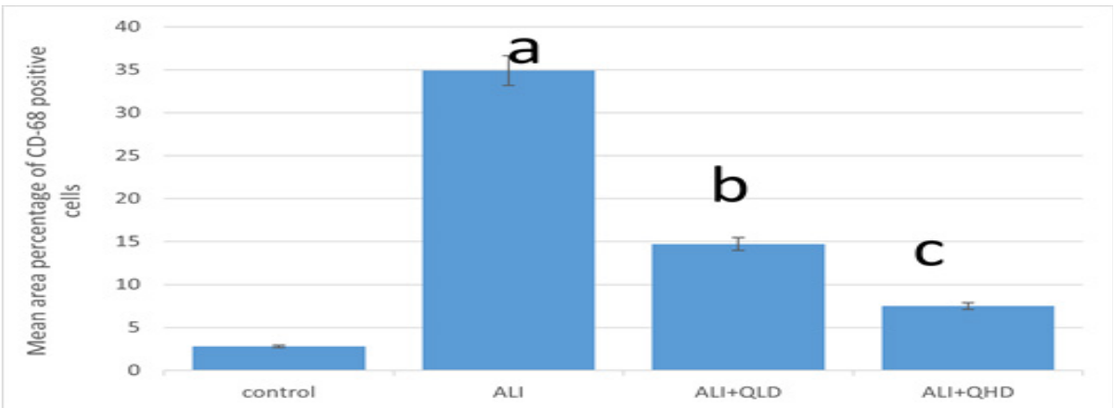

Histogram 2: The mean area percentage of CD68 positive cells in the immunohistochemical stained sections of lung.
Data expressed as mean ±standard deviatio
ALI: acute lung injury; ALI+QLD: acute lung injury+ quercetin low dose; ALI+QHD: acute lung injury + quercetin high dose
a: Highly significant increase compared to control group.
b: significant increase compared to control group and significant decrease compared to ALI group
c: non-significant increase compared to control group and highly significant decrease compared to ALI group.

Electron microscopic results

All control subgroups showed flat type I pneumocytes with flat nuclei. While, type II pneumocytes appeared cuboidal with euchromatic rounded nuclei. Their cytoplasm contained mitochondria, numerous lamellar bodies besides, a few short microvilli on their luminal surface. In addition, blood vessels lined by endothelial cells were seen (Figures 6A-C).

Fig. 6: Ultrastructure of the lung from the control group (6A) showing flattened type I pneumocyte (P1) with its flat nucleus (N) filling most of the cytoplasm. (6B) showing a type II pneumocyte (P2) which is cuboidal in shape with an euchromatic rounded nucleus (N), mitochondria (M), numerous lamellar bodies (L), and a few short microvilli on its luminal surface (arrowhead). (6C) showing flattened type I pneumocyte (arrow) with its flat nucleus filling most of the cytoplasm and blood capillary with normal endothelial lining (E) [Magnification;(6A–6C) ×2000. scale bar = 2 μm].

ALI-induced group exhibited type I pneumocytes with irregular nucleus. While type II pneumocytes showed nuclear indentation, degenerated mitochondria with destroyed cristae, many cytoplasmic vacuoles and empty lamellar bodies (L). The endothelium of the blood vessels had irregular, shrunk nucleus with nuclear membrane irregularities. In addition, the lumen of the blood vessels contained macrophage. Moreover, there was extravasation of RBCs and interstitial infiltrations with eosinophils (Figures 7A-F).

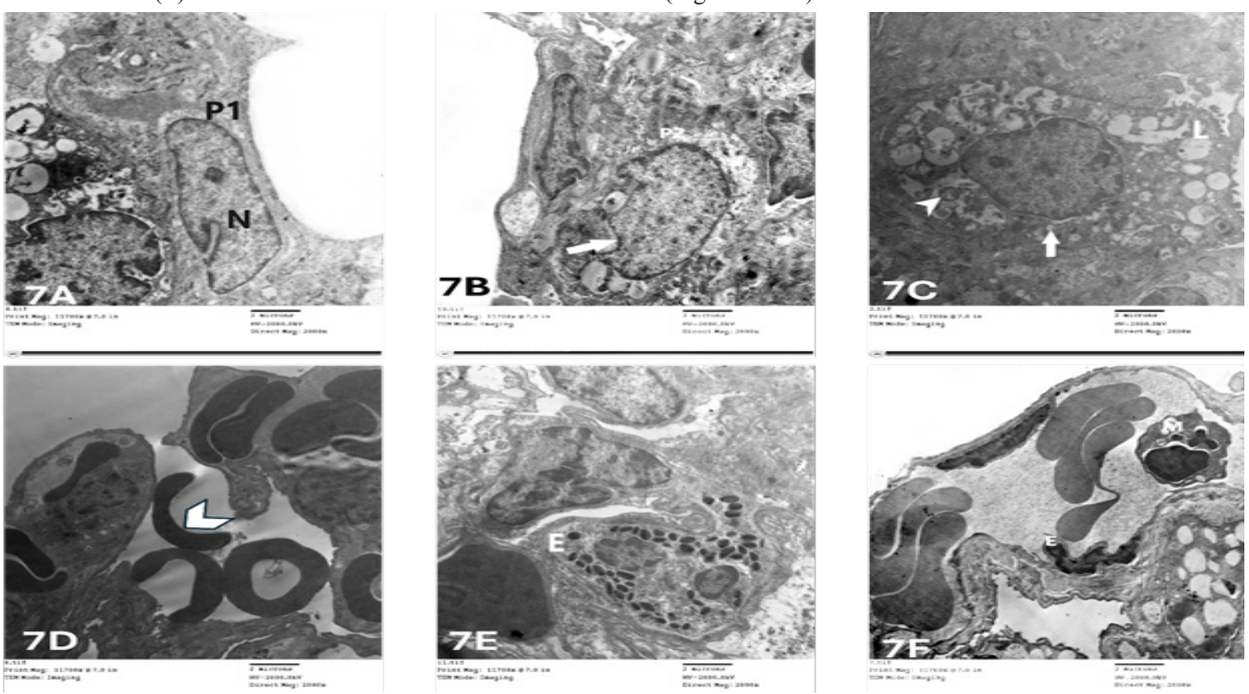

Fig. 7: ultrastructure of the lung from the ALI-induced group (7A) showing irregular shaped type I pneumocyte (P1) with irregular nucleus (N). Regarding type II pneumocyte (P2) (7B) showing nuclear indentation(arrow). Also (7C) has degenerated mitochondria and destroyed cristae (arrowhead), many cytoplasmic vacuoles (arrow) and empty lamellar bodies (L). (7D-7E) showing extravasation of RBCs (arrowhead) and interstitial infiltrations with eosinophils. (7F) shows blood capillary with its lining endothelium having irregular nucleus (arrow) and macrophage (M) inside its lumen [Magnification;(7A–7F) ×2000. scale bar = 2 μm].

In regard to subgroup IIIA (ALI+QLD), type I pneumocytes appeared normal. Whereas some of type II pneumocytes had nuclear indentation, abnormal shaped mitochondria, in addition to some empty lamellar bodies. Also, some blood vessels were lined with abnormal endothelium with nuclear membrane irregularities (Figures 8A-C).

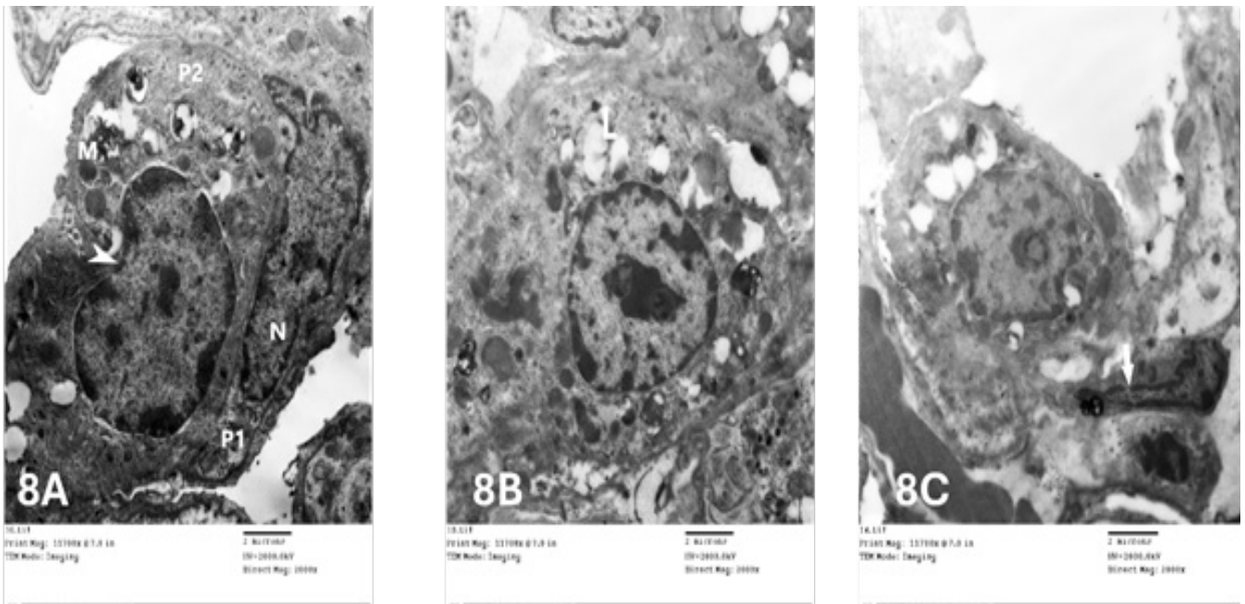

Fig. 8: Ultrastructure of the lung from Subgroup IIIA (ALI+QLD) (8A) showing type I pneumocyte (P1) with its flat nucleus (N) and type II pneumocyte (P2) with indented nucleus (arrowhead) and mitochondria(M). (8B) showing type II pneumocyte with some empty lamellar bodies (L). (8C) showing irregular endothelial cell with nuclear membrane irregularities (arrow) [Magnification;(8A–8C) ×2000. scale bar = 2 µm].

Regarding subgroup IIIB (ALI+QHD); it showed nearly normal ultrastructure of type I & II pneumocytes as well as blood vessels. As for type II pneumocytes; they showed refilled lamellar bodies (Figures 9A-C).

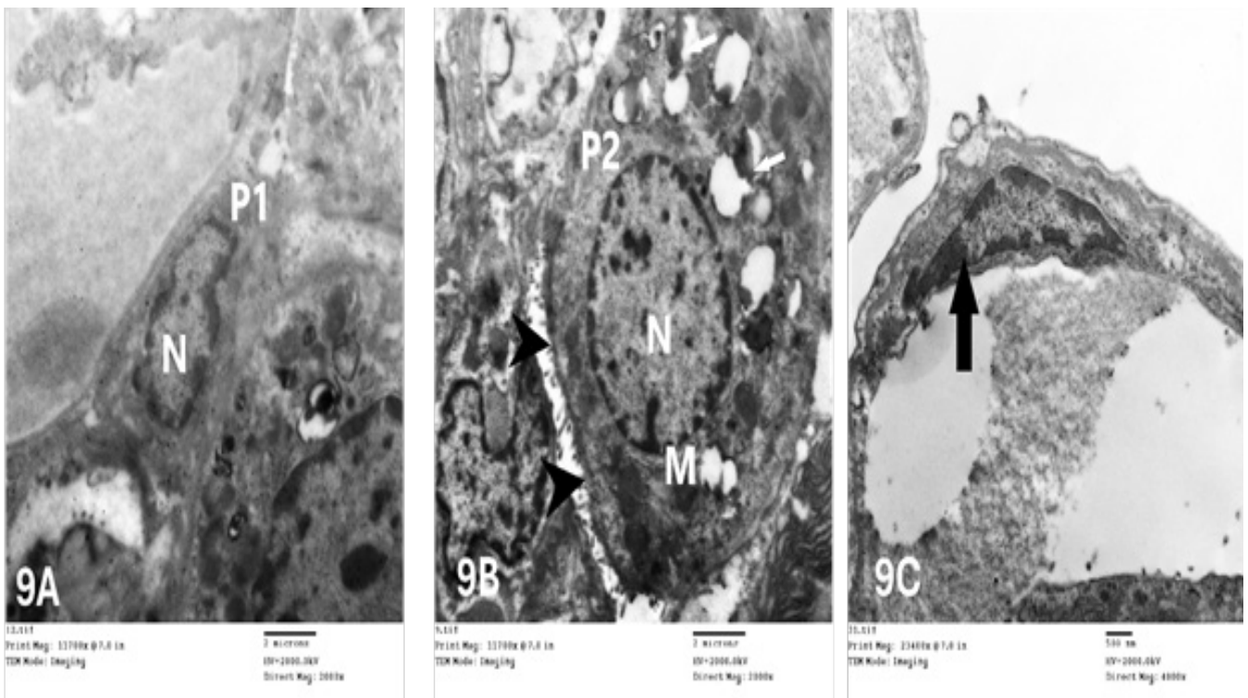

Fig. 9: Ultrastructure of the lung from Subgroup IIIB (ALI+QHD) (9A) showing type I pneumocyte with flattened nucleus. (9B) showing II pneumocyte (P2) with its euchromatic rounded nucleus(N), mitochondria (M)appeared more or less like control, refilling lamellar bodies(arrow) and microvilli on its luminal surface (arrowhead) [Magnification;(9A–9B) ×2000. scale bar = 2 µm]. (9C) showing a nearly normal blood capillary with its lining endothelium (arrow) [Magnification; ×4000. scale bar =500 nm].

DISCUSSION

Acute lung injury (ALI) is associated with manifestations of acute inflammation that could disrupt the lung endothelial and epithelial barriers. ALI can be manifested by severe hypoxemia, decreased lung activity with lost lung functions[20]. Most of the deaths of COVID-19 pandemic were attributed to ALI. Even though the molecular pathogenesis of ALI has recently been better understood, appropriate and efficient disease treatment has not yet been established[21].

The present OA model for acute lung injury was used to study the consequences of ALI, giving the hope for evaluating new treatment strategies[22]. Therefore, quercetin was used to assess its possible ameliorating effect on OA induced ALI.

In the present research, H&E results of ALI induced group (group II) showed disorganized alveoli, increase in the mean thickness of the interalveolar septae together with massive interstitial, and perivascular inflammatory cellular infiltrations, as well as the congested blood vessels, intra-alveolar and interstitial hemorrhage. These findings were in agreement with ***Kumar et al.***[23]. In accordance with ***Terzi et al.***[11] the destructive effect of OA on the lung tissue might be due to cytokine storms and oxidative stress. Oleic acid also impairs the balance between intracellular oxidant and the antioxidant defense system with upregulation of oxidative reactions with liberation of reactive oxygen species (ROS)[24].

Reactive oxygen species (ROS) lead to injured capillary endothelium due to liberation of super-oxides and malondialdehyde (MDA). These also lead to lipid peroxidation. Lipid peroxidation with lost functional integrity of cell membranes, consequently an increase in the alveolar-capillary permeability[25,26]. Meanwhile, the inflammatory cellular infiltrates could exacerbate the imbalance between the pro-inflammatory and anti-inflammatory responses, ending in increased cytokine release and damage to the lung vasculature[27].

In the current study, many of the bronchiolar epithelial cells of group II showed perinuclear vacuolation with detached cells and exudate inside its lumen. These results were in line with ***Neriman et al.***[28]. The significant bronchiolar morphological changes can be linked to the high susceptibility of its lining epithelial cells to oxidative stress leading to activated of autophagy and apoptosis pathways[29,30].

Cluster of differentiation 68 (CD68) is a lysosomal associated transmembrane glycoprotein produced by macrophages. It contributes to the activation and proliferation of T-lymphocyte[31]. Macrophages play a very important role in the pathophysiology of ALI. It liberates different cytokines, chemokines, and growth factors consequently, inflammation especially at the injured lungs[32].

Also, ALI induced group revealed a significant increase in the number and the mean area percentage of macrophages with positive cytoplasmic reaction for CD68 when compared to control group. It is consistent ***Ziablitsev et al.***[33]. This could be explained by the fact that macrophages' number increase secondary to the activation of inflammatory cascades by OA. Also, with the associated pulmonary oxidative stress; numerous cytokines would be released activating macrophages[34].

Ultrastructurally, the ALI group confirmed the light and immunohistochemical results with different changes of the lining alveoli. This might be due to the exposure to free radicals with disturbed lung biochemical processes ending by fluids and electrolyte imbalance[35,36].

Notably, type I pneumocytes were irregular with irregular nucleus, while type II pneumocytes had irregular indented nuclei and apparently enlarged mitochondria with destroyed cristae. These changes were attributed to the high level of ROS as well as associated lipid peroxidation affecting nuclear and mitochondrial membranes. So, DNA damage, and nuclear membranes irregularities ensued[37,38].

Moreover, type II pneumocytes of ALI group showed cytoplasmic vacuolations and areas of cytoplasmic rarefaction. These changes might be due to the degeneration of the cellular organelles by OS. In addition to misfolding of endoplasmic reticulum (ER) proteins with ER stress[39]. Moreover, the reduction in lipid transport and the accumulation of triglycerides in the cytoplasm could results into vacuolations[40].

In ALI group, type II pneumocytes had coalescent empty lamellar bodies. This could be explained by the fact that acute lung inflammation leads to impaired synthesis, secretion, and composition of surfactant proteins[41]. Furthermore, ALI group showed irregular endothelial cells with irregular nuclei and extravasation of RBCs which might be due to glycocalyx degradation, oxidative stress and inflammation induced by OA[42].

In this work, the administration of quercetin reduces lung tissue inflammation and improves the histological architecture in dose-dependent manner. The ALI+QLD group showed moderate interstitial hemorrhage and some thickening of the interalveolar septae associated with small areas of interstitial and perivascular cellular infiltrations. While ALI+QHD group revealed nearly normal structure which was consistent with the study of ***Omar et al.***[43]. This improvement could be explained by the antioxidant effect of quercetin which protects against cell damage. Quercetin reduces ROS and MDA production, enhances cell state, and upregulates autophagy[44,45]. Moreover, it upregulates the nuclear factor erythroid 2–related factor 2 (Nrf2) driven antioxidant production, alleviating the oxidative stress[46].

Furthermore, quercetin has an anti-inflammatory effect through downregulating the expression of different pro-inflammatory cytokines such as IL-6, IL-8, TNF-α, IL-1β, and monocyte chemoattractant protein-1 (MCP-1) that are produced by macrophages, and peripheral blood mononuclear cells. It also inhibits the release of different inflammatory chemicals like phospholipase A, cyclooxygenase, and arachidonic acid[47].

Moreover, quercetin subgroups showed dose dependent significant reduction in the mean number of macrophages positive for CD68. These results are coincided with ***Peng et al.***[48] who discovered that quercetin can reduce macrophage damage through enhancing the antioxidant activity in addition to down regulating the released inflammatory factors. Quercetin also reduce the synthesis of NO, proinflammatory cytokine expression, and lipocalin-2 as well as the production of chemokines, CCL2, and CXCL10[49].

On the ultrastructure level, lung sections from the quercetin treated group showed also dose dependent improvement. Quercetin inhibits the opened mitochondrial permeability transition pores (mPTP) with the alleviation of different cellular degenerative changes[50]. Furthermore, quercetin is connected to the mitochondrial DNA replication and oxidative phosphorylation via PGC-1α (Peroxisome proliferator activated receptor gamma coactivator1-alpha), a co-activator of genes[51]. Additionally, quercetin increases Keap1/Nrf2 expression (self-anti-oxidative stress pathway) improving endothelial cell functions[52].

Taken altogether, it could be concluded that quercetin has an ameliorating effect on the histological structure of the lung tissue in acute lung injury model of adult male albino rats in dose dependent manner. So, quercetin may be useful in the treatment of acute lung injury especially when used in a high dose.

CONFLICT OF INTERESTS

There is no conflicts of interest.

FUNDING

There was no funding for the study from any source.

REFERENCES

1. **Hu, Y., C. Ciminieri, Q. Hu, M. Lehmann, M.** Königshoff and R. Gosens. "WNT Signalling in Lung Physiology and Pathology." Handb Exp Pharmacol.2021;269: 305-336.

2. **Gonçalves-de-Albuquerque, C. F., A. R. Silva, P. Burth, M. V. Castro-Faria and H. C. Castro-Faria-Neto.** "Acute Respiratory Distress Syndrome: Role of Oleic Acid-Triggered Lung Injury and Inflammation." Mediators Inflamm 2015; 260465.

3. **Akella, A., P. Sharma, R. Pandey, and S. B. Deshpande.** "Characterization of oleic acid-induced acute respiratory distress syndrome model in rat." Indian J Exp Biol. 2014;52 (7): 712-9.

4. **Sharma, P., R. Pandey, and S. B. Deshpande.** 2016. "Indomethacin Exacerbates Oleic acid-induced acute respiratory distress syndrome in adult rats." Indian J Physiology Pharmacology 60 (1): 82-9.

5. **Obiol, D. J., M. J. Amundarain, F. Zamarreño, A. Vietri, S. S. Antollini and M. D. Costabel.** "Oleic Acid Could Act as a Channel Blocker in the Inhibition of nAChR: Insights from Molecular Dynamics Simulations." The Journal of Physical Chemistry B.2024;128(10): 2398-2411.

6. **Zhang, J., Y. Guo, M. Mak and Z. Tao.** "Translational medicine for acute lung injury." Journal of Translational Medicine.2024; 22(1): 25.

7. **Takashima, K., M. Matsushima, K. Hashimoto, H. Nose, M. Sato, N. Hashimoto, Y. Hasegawa, and T. Kawabe.** "Protective effects of intratracheally administered quercetin on lipopolysaccharide-induced acute lung injury." Respir Res.2014 ;15 (1): 150.

8. **Magar, R. T. and J. K. Sohng.** "A Review on Structure, Modifications and Structure-Activity Relation of Quercetin and Its Derivatives." J Microbiol Biotechnol.2020; 30(1): 11-20.

9. **Yang, H. Li, B. Hao, D. Cui, R. Shang, Y. Lv, Y. Liu, W. Pu, H. Zhang, J. He, X. Wang and S.** Wang "Quercetin Reprograms Immunometabolism of Macrophages via the SIRT1/PGC-1α Signaling Pathway to Ameliorate Lipopolysaccharide-Induced Oxidative Damage." International Journal of Molecular Sciences 24.2023; DOI: 10.3390/ijms24065542.

10. **El-Said, K. S., A. Atta, M. A. Mobasher, M. O. Germoush, T. M. Mohamed and M. M. Salem.** "Quercetin mitigates rheumatoid arthritis by inhibiting adenosine deaminase in rats.2022;" Mol Med 28(1): 24.

11. **Terzi, F., B. Demirci, İ. Çınar, M. Alhilal and H. S. Erol.** "Effects of tocilizumab and dexamethasone on the downregulation of proinflammatory cytokines and upregulation of antioxidants in the lungs in oleic acid-induced ARDS." Respir Res.2022; 23(1): 249.

12. **Verma, R., L. Kushwah, D. Gohel, M. Patel, T. Marvania and S. Balakrishnan.** "Evaluating the Ameliorative Potential of Quercetin against the Bleomycin-Induced Pulmonary Fibrosis in Wistar Rats." Pulm Med 2013: 921724.

13. **Abdel Aziz, R. L., A. Abdel-Wahab, F. I. Abo El-Ela, N. E. Y. Hassan, E. S. El-Nahass, M. A. Ibrahim and A. A. Y. Khalil.** "Dose- dependent ameliorative effects of quercetin and l-Carnitine against atrazine-induced reproductive toxicity in adult male Albino rats." Biomed Pharmacother.2018;102: 855-864.

14. **Laferriere, C. A. and D. S. Pang.** "Review of Intraperitoneal Injection of Sodium Pentobarbital as a Method of Euthanasia in Laboratory Rodents." J Am Assoc Lab Anim Sci. 2020;59(3): 254-263.

15. **Alturkistani, H. A., F. M. Tashkandi and Z. M. Mohammedsaleh.** "Histological Stains: A Literature Review and Case Study." Glob J Health Sci.2015; 8(3): 72-79.

16. **Arkhipov, S.** Protocol for immunohistochemistry (IHC) staining of paraffinized tissues with anti-CD68 antibody.2020;

17. **Graham, L. and J. M. Orenstein.** "Processing tissue and cells for transmission electron microscopy in diagnostic pathology and research." Nature Protocols.2007; 2(10): 2439-2450.

18. **Li, M., S. Lu, P. Huang, T. Xia, Z. Yu, W. Jiang, Y. Mao, C. Yang, S. Yu, W. Wu and Y. Zhang.** "High-quality, large-scale, semi-thin, & ultra-thin sections of the optic nerve in large animals: An optimized procedure." Experimental Eye Research.2022; 219: 108956.

19. **Mousa, H., Abdelfadeel, K., Hassan, M.** 'Green Kiwi Fruit Extract Ameliorates Aspartame Toxicity on the Lung of Adult Male Abino Rat (Histological and Immunohistochemical Study)', Journal of Medical Histology, 3(2), pp. 192-205. doi: 10.21608/jmh.2019.15854.1063

20. **Tian, C., P. Zhang, J. Yang, Z. Zhang, H. Wang, Y. Guo and M. Liu.** "The protective effect of the flavonoid fraction of Abutilon theophrasti Medic. leaves on LPS-induced acute lung injury in mice via the NF-κB and MAPK signalling pathways." Biomed Pharmacother.2019; 109: 1024-1031.

21. **Li, L., Q. Huang, D. C. Wang, D. H. Ingbar and X. Wang.** "Acute lung injury in patients with COVID-19 infection." Clin Transl Med.2020; 10(1): 20-27.

22. **Zhang, J., Y. Guo, M. Mak and Z. Tao.** "Translational medicine for acute lung injury." Journal of Translational Medicine 2024;22(1): 25.

23. **Kumar, S., P. Bhagat, S. Pandey and R. Pandey.** "The Role of Antioxidant Agent (N-Acetylcysteine) in Oleic Acid-Induced Acute Lung Injury in a Rat Model." Cureus.2022;14(9): e29478.

24. **Ali, H., A. Khan, J. Ali, H. Ullah, A. Khan, H. Ali, N. Irshad and S. Khan.** "Attenuation of LPS-induced acute lung injury by continentalic acid in rodents through inhibition of inflammatory mediators correlates with increased Nrf2 protein expression." BMC Pharmacology and Toxicology.2020; 21(1): 81.

25. **Bezerra, F. S., M. Lanzetti, R. T. Nesi, A. C. Nagato, C. P. e. Silva, E. Kennedy-Feitosa, A. C. Melo, I. Cattani-Cavalieri, L. C. Porto and S. S. Valenca.** "Oxidative Stress and Inflammation in Acute and Chronic Lung Injuries." Antioxidants 2023, Vol. 12, Page 548 12(3): 548-548.

26. **Mishra, P., R. Pandey, N. Pandey, S. Tripathi and Y. B. Tripathi (2022).** "Prevention of mortality in acute lung injury induced by oleic acid: Application of polyherbal decoction (bronco T)." Front Cell Dev Biol.2022;10: 1003767.

27. **Qiao, X., J. Yin, Z. Zheng, L. Li and X. Feng.** "Endothelial cell dynamics in sepsis-induced acute lung injury and acute respiratory distress syndrome: pathogenesis and therapeutic implications." Cell Communication and Signaling.2024;22(1): 241.

28. **Neriman, A., A. Pergin, I. Alper Bektas and T. Arzu.** "Long-Term Simvastatin Attenuates Lung Injury and Oxidative Stress in Murine Acute Lung Injury Models Induced by Oleic Acid and Endotoxin." Respiratory Care.2011;56(8): 1156.

29. **Sunil, V. R., K. N. Vayas, C. B. Massa, A. J. Gow, J. D. Laskin and D. L. Laskin.** "Ozone-Induced Injury and Oxidative Stress in Bronchiolar Epithelium Are Associated with Altered Pulmonary Mechanics." Toxicological Sciences.2013; 133(2): 309-319.

30. **Kandeel, S. and R. S. Estfanous (2022).** "The Possible Protective Effect of Magnolol on Triolein-Induced Lung Structural Changes in Rats: Histological and Immunohistochemical Study." Egyptian Journal of Histology.2022; 45(2): 359-371.

31. **Chen, R., D. Yang, L. Shen, J. Fang, R. Khan and D. Liu.** "Overexpression of CD86 enhances the ability of THP-1 macrophages to defend against Talaromyces marneffei." Immun Inflamm Dis.2022;10(12): e740.

32. **Osorio-Valencia, S. and B. Zhou** "Roles of Macrophages and Endothelial Cells and Their Crosstalk in Acute Lung Injury." Biomedicines 12.2024; DOI: 10.3390/biomedicines12030632.

33. **Ziablitsev, D. S., M. Kozyk, K. Strubchevska, O. O. Dyadyk and S. V. Ziablitsev.** "Lung Expression of Macrophage Markers CD68 and CD163, Angiotensin Converting Enzyme 2 (ACE2), and Caspase-3 in COVID-19." Medicina (Kaunas).2023; 59(4).

34. **Guan, T., X. Zhou, W. Zhou and H. Lin (2023).** "Regulatory T cell and macrophage crosstalk in acute lung injury: future perspectives." Cell Death Discovery.2023;9(1): 9.

35. **Albanawany, N. M., D. M. Samy, N. Zahran, R. M. El-Moslemany, S. M. Elsawy and M. W. Abou Nazel (2022).** "Histopathological, physiological and biochemical assessment of resveratrol nanocapsules efficacy in bleomycin-induced acute and chronic lung injury in rats." Drug Delivery 29(1): 2592-2608.

36. **Hafez, S. M. N. A., E. A. Saber, N. M. Aziz, M. Y. Kamel, A. A. Aly, E.-S. M. N. Abdelhafez and M. F. G. Ibrahim.** "Potential protective effect of 3,3′-methylenebis(1-ethyl-4-hydroxyquinolin-2(1H)one)against bleomycin-induced lung injury in male albino rat via modulation of Nrf2 pathway: biochemical, histological, and immunohistochemical study." Naunyn-Schmiedeberg's Archives of Pharmacology.2023; 396(4): 771-788.

37. **Juan, C., J. Perez de la lastra, F. Plou and E. Lebeña.** "The Chemistry of Reactive Oxygen Species (ROS) Revisited: Outlining Their Role in Biological Macromolecules (DNA, Lipids and Proteins) and Induced Pathologies." International Journal of Molecular Sciences.2021;22: 4642.

38. **Bashandy, M. A. And O. I. Zedan.** "Role of Alpha Lipoic Acid on Cyclophosphamide Induced Cardiotoxicity in Adult Male Albino Rat: Histological Study." Egyptian Journal of Histology.2019; 42(4): 888-899.

39. **Solaiman, A., R. A. Mehanna, G. A. Meheissen, S. Elatrebi, R. Said and N. H. Elsokkary.** "Potential effect of amniotic fluid-derived stem cells on hyperoxia-induced pulmonary alveolar injury." Stem Cell Research & Therapy.2022;13(1): 145.

40. **Chen, Ze, Ruifeng Tian, Zhigang She, Jingjing Cai, and Hongliang Li.** "Role of oxidative stress in the pathogenesis of nonalcoholic fatty liver disease." Free Radical Biology and Medicine 152 (2020): 116-141.

41. **Aly, A. A., A. A. Hassan, A. H. Mohamed, E. M. Osman, S. Bräse, M. Nieger, M. A. A. Ibrahim and S. M. Mostafa (2021).** "Synthesis of 3,3′-methylenebis(4-hydroxyquinolin-2(1H)-ones) of prospective anti-COVID-19 drugs." Molecular Diversity. 2021;25(1): 461-471.

42. **Tenghao, S., M. Shenmao, W. Zhaojun, B. Jijia, Z. Wenjie, Z. Wenyan and M. Xigang.** "Keratinocyte Growth Factor-2 Is Protective in Oleic Acid-Induced Acute Lung Injury in Rats." Evid Based Complement Alternat Med 2019: 9406580.

43. **Omar, S., M. M. Abd ElAziz and M. M. Mady.** "Protective Role of Quercetin in Preventing Thioacetamide Induced Heart and Lung Injury in Adult Male Albino Rat." Egyptian Journal of Histology.2023;46(4): 1837-1746.

44. **Chen, B. H., J. H. Park, J. H. Ahn, J. H. Cho, I. H. Kim, J. C. Lee, M. H. Won, C. H. Lee, I. K. Hwang, J. D. Kim, I. J. Kang, B. N. Shin, Y. H. Kim, Y. L. Lee and S. M. Park.** "Pretreated quercetin protects gerbil hippocampal CA1 pyramidal neurons from transient cerebral ischemic injury by increasing the expression of antioxidant enzymes." Neural Regen Res.2017; 12(2): 220-227.

45. **Yu, P.-R., C.-Y. Tseng, C.-C. Hsu, J.-H. Chen and H.-H. Lin.** "In vitro and in vivo protective potential of quercetin-3-glucuronide against lipopolysaccharide-induced pulmonary injury through dual activation of nuclear factor-erythroid 2 related factor 2 and autophagy." Archives of Toxicology.2024;98(5): 1415-1436.

46. **Boots, A. W., C. Veith, C. Albrecht, R. Bartholome, M.-J. Drittij, S. M. H. Claessen, A. Bast, M. Rosenbruch, L. Jonkers, F.-J. van Schooten and R. P. F. Schins.** "The dietary antioxidant quercetin reduces hallmarks of bleomycin-induced lung fibrogenesis in mice." BMC Pulmonary Medicine.2020; 20(1): 112.

47. **Al-Khayri, J. M., G. R. Sahana, P. Nagella, B. V. Joseph, F. M. Alessa and M. Q. Al-Mssallem.** "Flavonoids as Potential Anti-Inflammatory Molecules: A Review." Molecules.2022; 27(9).

48. **Peng, J., Z. Yang, H. Li, B. Hao, D. Cui, R. Shang, Y. Lv, Y. Liu, W. Pu, H. Zhang, J. He, X. Wang and** S. Wang "Quercetin Reprograms Immunometabolism of Macrophages via the SIRT1/PGC-1α Signaling Pathway to Ameliorate Lipopolysaccharide-Induced Oxidative Damage." International Journal of Molecular Sciences.2023; 24 DOI: 10.3390/ijms24065542.

49. **Tsai, C. F., G. W. Chen, Y. C. Chen, C. K. Shen, D. Y. Lu, L. Y. Yang, J. H. Chen and W. L. Yeh.** "Regulatory Effects of Quercetin on M1/M2 Macrophage Polarization and Oxidative/Antioxidative Balance." Nutrients.2021; 14(1).

50. **Ferenczyova, K., B. Kalocayova and M. Bartekova.** "Potential Implications of Quercetin and its Derivatives in Cardioprotection." Int J Mol.2020;Sci 21(5).

51. **Rasheed, R., M. Othman, U. Hussein and a. embaby.** "The Possible Ameliorative Influence of Quercetin on Cardiac Muscle Changes induced by High Fat Diet in Adult Male Albino Rats: Light and Electron Microscopic Study." Egyptian Journal of Histology.2022; 45(3): 937-948.

52. **Zamanian MY, Soltani A, Khodarahmi Z, Alameri AA, Alwan AMR, Ramírez-Coronel AA, Obaid RF, Abosaooda M, Heidari M, Golmohammadi M, Anoush M.** Targeting Nrf2 signaling pathway by quercetin in the prevention and treatment of neurological disorders: An overview and update on new developments. Fundam Clin Pharmacol. 2023 Dec;37(6):1050-1064. doi: 10.1111/fcp.12926. Epub 2023 Jun 16. PMID: 37259891.

دور الكيرستين فى تحسين التغيرات النسيجية لنموذج إصابة الرئة الحادة للجرذ: دراسة هستولوجية وهستوكيمائية مناعية

نهال أحمد دويدار، سماح قنديل السيد قنديل، نادية فؤاد السيد أبو حسن و هبه السيد محمد شرف الدين

قسم الهستولوجيا و بيولوجيا الخلية، كلية الطب، جامعة طنطا

الخلفية: الإصابة الرئوية الحادة تكون مرتبطة بإلتهاب حاد وشديد يتسبب فى تعطيل الحاجز الطلائي و الخلايا المبطنة لجدران الأوعية الدموية للرئة. تم استخدام حمض الأوليك لإستحداث نموذج التهاب رئوى حاد فى الجرذان. الكيرسيتين هو فلافونويد له خصائص مضادة للإلتهابات ومضادة للأكسدة.

الهدف: أجرى هذه البحث لدراسة دورالكيرسيتين على تحسن التغييرات النسيجية لنموذج إصابة الرئة الحادة للجرذ بإستخدام تقنيات هستولوجية وهستوكيميائية مناعية.

مادة وطرق البحث: تم تقسيم ٤٨ من ذكور الجرذان البيضاء البالغة (٢٠٠ - ٢٥٠ جرام، ٨ - ٩ أسابيع) إلى:

المجموعة الأولى (المجموعة الضابطة)

المجموعة الثانية (نموذج الإلتهاب الرئوي الحاد) تناولت ٥٠ ميكرولتر من حمض الأوليك المذاب في ١٪ من زلال مصل البقر عن طريق وريد الذيل.

المجموعة الثالثة: ١٦ جرذاً تناولوا حمض الأوليك مثل المجموعة الثانية ثم تم تقسيمها إلى: المجموعة الفرعية(٣أ) والمجموعة الفرعية (٣ب): تناولت الجرذان ١٠و ٥٠ مج/كجم من الكيرسيتين عن طريق الفم يوميًا لمدة ٢١يوما.

النتائج: أظهرت (مجموعة الإلتهاب الرئوي الحاد) تضخم في الحاجز بين الحويصلات الهوائية و تجمع خلايا إلتهابية فى النسيج البينى للرئة وحول الأوعية الدموية وإحتقان الأوعية الدموية مع عدم إنتظام الحويصلات الهوائية مع وجود نزيف داخل الحويصلات وفي النسيج البينى للرئة.

بالنسبة للقصيبات الهوائية، ظهرت الخلايا الطلائية غير مترابطة ومصحوبة بتكيسات حول النواة ووجود إفرازات داخل تجويفها. وكان كل ذلك مرتبطًا بمناطق ذات حمضية متجانسة وأيضاً زيادة ذات دلالة إحصائية في المساحة التى تشغلها الخلايا ذات رد فعل سيتوبلازمى إيجابي لCD٨٦.

بجانب، تغييرات بارزة في هيكل خلايا الرئة من النوع الأول والثاني و الشعيرات الدموية بالرئة. (مجموعة علاج الكيرستين) أظهرت تحسنًا في التركيب النسيجي للرئة اعتماداً على الجرعة.

الإستنتاج: الكيرسيتين يحسن من الإلتهاب الرئوي الحاد اعتماداً على جرعته.